

# Integration of Single Atoms for Tandem Catalysis

Cun Liu, Botao Qiao,\* and Tao Zhang\*



Cite This: *JACS Au* 2024, 4, 4129–4140

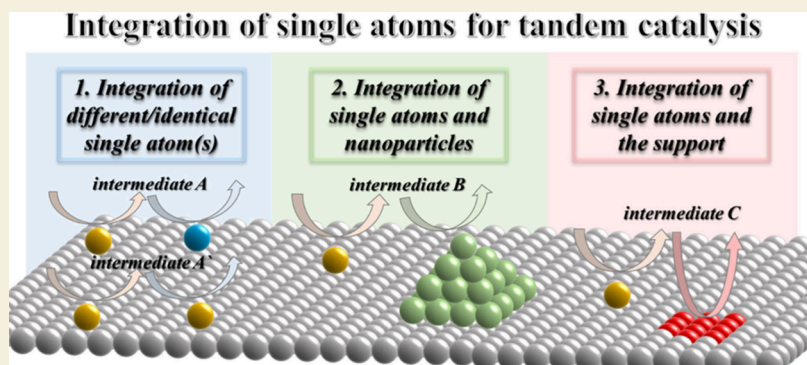


Read Online

ACCESS |

Metrics & More

Article Recommendations



**ABSTRACT:** Tandem catalysis represents an efficient pathway which greatly saves the overall facilities and energy inputs. The intermediates are transported from one active site to the other site more efficiently due to the ease of mass transfer in one reactor system. However, sometimes the indiscriminate usage of this concept can be misleading, and thereby, this Perspective first aims for differentiating “tandem catalysis” from liable-to-muddling concepts, such as “synergy” and “domino/cascade catalysis.” The prerequisites for figuring out tandem catalysis mainly lie in (1) the two or more independent catalytic cycles involved in one system, where the products of one reaction cycle can be immediately relayed to a subsequent reaction cycle as the reactants, and (2) these cycles occurring in different catalytic mechanisms. As a frontier in heterogeneous catalysis, single-atom catalysts possess the unique property of high selectivity toward transformation of specific chemical bonds and can also bridge the homo- and heterogeneous catalysis. However, despite their wide range of applications, single-atom catalysts (SACs) are not solutions to all catalytic processes, particularly those reactions requiring active sites containing multiatoms in their proximity. To this end, the strategy of combining SACs within tandem processes is a feasible way to broaden the scope of chemical reactions achievable over SACs. Therein, according to the category of the participating active species, four subsections are thoroughly introduced, including tandem catalysis over the integration of (1) different/identical single atom(s), (2) single atoms and nanoparticles, and (3) single atoms and the adjacent support. Nonetheless, with regard to the investigation of the involved single-atom catalysts, some issues still remain regarding the exact characterization and explicit comparison of catalytic performance with that over their nanoparticle counterparts. Moreover, some intriguing subjects are still waiting to be systematically explored to broaden and deepen single-atom-integrated tandem processes in the branch of catalytic science.

**KEYWORDS:** *Single-atom catalysts, Tandem catalysis, Heterogeneous catalysis, Synergy, Cascade catalysis*

## 1. INTRODUCTION

As the ever-existing paradigm, spontaneous chemical reactions in nature tend to occur in ways in which entropy increases with optimized atom economy and energy consumption. As for human activities, modern chemical industries need to exploit reaction engineering to attain highly efficient reaction processes for the balance between financial costs and upgrading of raw chemicals. Thus, from the perspective of improving the efficiency of catalytic transformations, integration of multiple reaction processes in just one pot is a feasible approach and it saves the overall facilities and energy inputs. Meanwhile, the intermediates are transported from one active site to the other site more efficiently due to the ease of mass

transfer in one reactor system. Therein, tandem catalysis, which encompasses two or more mechanistically independent catalytic cycles in one system, where the products of one reaction can be immediately relayed to a subsequent reaction as the reactants,<sup>1,2</sup> is a versatile toolkit for consecutively transforming raw materials to the targeted chemicals. Tandem

**Received:** August 27, 2024  
**Revised:** September 22, 2024  
**Accepted:** September 25, 2024  
**Published:** October 30, 2024



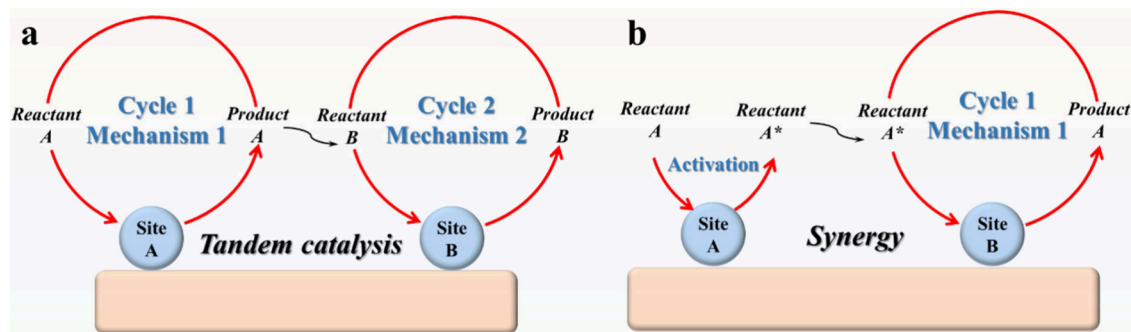


**Figure 1.** Illustrative demonstrations of (a) tandem catalysis and (b) catalytic synergy processes. Note: the concept of synergy is a general term that can widely refer to the cooperation between different active sites or components to enhance the overall catalytic performance. Here, Figure 1b just take one scenario for example, where site A can complement the whole reaction occurred on site B by fostering the adsorption and activation of the reactant.

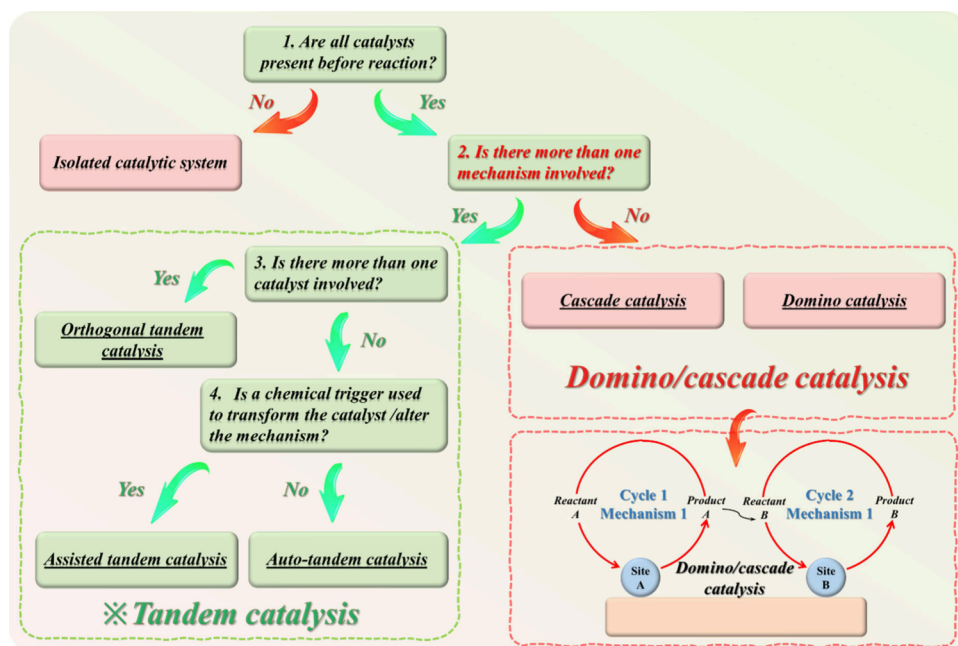


**Figure 2.** Flowchart to guide the nomenclature of multiple catalytic transformations in one pot. The contents in lower right dashed box describes the catalytic cycles during the domino/cascade processes. Note: this flowchart is partially referenced and redesigned based on ref 1.

catalysis not only offers an attractive choice as sustainable processes with high atom utilization and minimized loss of reagents,<sup>3</sup> but also provides a prospective platform for the possibility of exploring innovative synthetic routes.

#### Tandem Catalysis or Synergy?

Bearing the above merits, tandem catalysis is becoming more and more practical, thanks to the integration of compatible reactions in thermodynamics/kinetics. However, the usage of this concept is sometimes obscure and misleading, thus needing clarification with some common but confusing terminology, such as synergy. As shown in Figure 1a, the tandem catalysis process needs to involve the coupling of sequential transformation cycles with different mechanisms,<sup>4,5</sup> during which the reactant of the second cycle is directly transferred from the first cycle (product A  $\rightarrow$  reactant B in Figure 1a). Before the brief discussion on the concept of synergy, we would like to clarify that this general term can widely refer to the cooperation between different active sites or components to enhance the overall catalytic performance. But here we just take one case for example, where one site (site A)

can complement the whole reaction occurred on the other site (site B) in a synergetic manner by fostering the adsorption and activation of the certain reactant (Figure 1b). In this scenario, the reaction cycle still occurs on site B even without site A. Compared with the conventional configuration with single active sites that are accountable for both reactant activation and transformation, the synergetic mode unequivocally improves the catalytic efficiency due to the smaller “workload” on catalytic active site,<sup>6</sup> i.e., site B in Figure 1b. For instance, Ni and Ru single atoms have been successfully anchored on CeO<sub>2</sub> nanorods for the dry reforming of CH<sub>4</sub>, during which Ni and Ru single atoms are responsible for the activation of CH<sub>4</sub> and CO<sub>2</sub>, respectively.<sup>7</sup> In comparison with the traditional single Ni site, the as-obtained dual Ni–Ru catalyst definitely exhibits more than twice the turnover frequency in the temperature range 500–560 °C. Therefore, the prerequisite to distinguish “tandem catalysis” with “synergy” is to ascertain whether the coupling of sequential catalytic cycles with different mechanisms exists. Sometimes, there can be overlaps between tandem and synergistic processes because the active

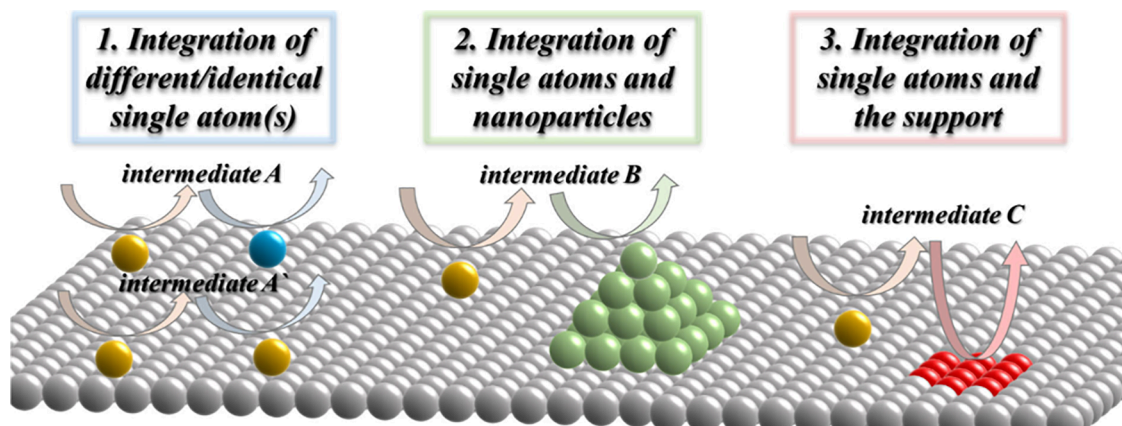


**Figure 3.** Schematic illustration of the integration of single atoms with other active sites in tandem catalysis. Note: the intermediate refers to the product that is formed during the first catalytic cycle and then transferred to the second catalytic cycle as the reactant.

sites not only function sequentially but also enhance each other's performance in a synergistic manner. Moreover, it is worthwhile to briefly mention that, apart from catalytic synergy, the conception of "bifunctional catalysis" is also reasonable for describing synchronous activations of substrates at complementary active sites,<sup>8</sup> which is the case of recent published Rh-WO<sub>x</sub> pair site catalysts for ethylene hydroformylation by the group of Christopher.<sup>9</sup>

#### Tandem Catalysis or Domino/Cascade Catalysis?

Apart from distinguishing the "tandem catalysis" with frequently mentioned notions of "synergetic" and "bifunctional" active sites, there are also other parallel branches with and/or subgroups of tandem catalysis emphasizing to be clarified, such as domino or cascade catalysis.<sup>10</sup> For a more explicit illustration, Figure 2 delineates the flowchart that the relevant researchers need to check to ensure the appropriate usage of nomenclatures. As referred above, the prerequisites for tandem catalysis are sequentially occurring mechanistically distinct reaction cycles in just one pot (Figure 2, Nos. 1 and 2). Otherwise, the sequentially catalytic cycles bearing identical mechanisms (Figure 2, lower right dashed box), such as (1) the hydrogenation of acetylene to the desired ethylene and the following overhydrogenation to ethane<sup>11</sup> and (2) the dehydrogenation of cyclohexanol to cyclohexanone and successive to phenol,<sup>12</sup> are referred to as cascade or domino catalysis (Figure 2, No. 3). With regard to the branch of tandem catalysis, the subordinate catalytic system of orthogonal tandem catalysis requires more than one catalyst/active site to relay the consecutive processes (Figure 2, No. 3), while the nonorthogonal tandem catalysis can be further classified as assisted and autotandem catalysis depending on whether a chemical trigger is highly necessary to alter the catalytic mechanism amid the intermediate transformations (Figure 2, No. 4), which are beyond the scope of this Perspective. Therein, the aim to differentiate between tandem and domino/cascade catalysis is to discern the number of involved catalytic mechanisms during the multiple reaction cycles.

#### Integration of Single-Atom Catalysts for Tandem Catalysis

Single-atom catalysts (SACs) have triggered tremendous attention since the concept was put forward<sup>13</sup> because of the theoretically maximum atom utilization and intrinsic catalytic behaviors different from those of nanocatalyst counterparts. The mononuclear and isolated atoms can drastically alter the adsorption configurations/capacities and activation mecha-

nisms of the reactants: on the one hand, the isolated atom merely interacts with one functional group in a single reaction cycle due to the limited active sites compared with the multiple sites in nanoparticulate counterparts, thus fostering the selective transformation of reactants to the aiming products, such as the selective hydrogenation of 1,3-butadiene to 1-butene over Pd single atoms in contrast with the overhydrogenation to butane over Pd nanoparticles;<sup>14</sup> on the other hand, due to the absence of adjacent metal sites, the isolated atom tends to change the dissociation pattern of molecular H<sub>2</sub> from homolytic dissociation over nanoparticles to the heterolytic dissociation, resulting in the prioritized hydrogenation of polar unsaturated bonds such as selective hydrogenation of C=O in cinnamaldehyde.<sup>15</sup> In addition, single-atom catalysts are also considered to bridge the homo- and heterogeneous catalysis for the similarly mononuclear active sites but are meanwhile more feasible to separate and further reuse. The heterogenization of homogeneous catalysis has already been investigated, for example, in Suzuki coupling, hydroformylation, hydrosilylation, and boronation.<sup>16–19</sup> However, despite their wide range of applications, SACs are not solutions to all catalytic processes, particularly those reactions requiring active sites containing multiatoms in proximity. To this end, the strategy of combining SACs within tandem processes is a feasible way to broaden the scope of chemical reactions achievable over SACs.

In this Perspective, we focus on the integration of SACs in tandem catalysis. As illustrated in Figure 3, four parts are presented in the next section based on the kind of involved active sites, including tandem catalysis over the integration of (1) different/identical single atom(s), (2) single atoms and nanoparticles, and (3) single atoms and the adjacent support. Yet it is worth noting that type (1) of the different single atoms, (2) and (3), all belong to orthogonal tandem catalysis while the identical single-atom-catalyzing process undoubtedly is the nonorthogonal one. Moreover, we also describe some persistent issues upon the integration of single atoms in tandem catalysis and the perspectives for possible future development in the relevant fields.

Table 1. Tandem Catalysis over Different/Identical Single Atom(s)

Entry	Catalyst	Tandem path <sup>a</sup>	Key results	Ref
1	Ru <sub>1</sub> /CeO <sub>2</sub> & Rh <sub>1</sub> /CeO <sub>2</sub>	Isomerization (Ru <sub>1</sub> ) + hydrosilylation (Rh <sub>1</sub> )	Regioselectivity > 95% for terminal organosilane compounds from olefin isomers	20
2	Rh <sub>1</sub> @S-1	<i>In-situ</i> H <sub>2</sub> generation (Rh <sub>1</sub> ) + hydrogenation (Rh <sub>1</sub> )	Yield > 99% for amine and shape-selective for p- nitroarenes	21
3	Co SSCs@NG-800–50	<i>In-situ</i> H <sub>2</sub> generation (CoN <sub>3</sub> ) + hydrogenation (CoN <sub>3</sub> )	Nitrobenzene conversion > 99% and 96.3% aniline selectivity	22
4	Rh <sub>1</sub> /HAP	Hydroformylation (Rh <sub>1</sub> ) + Hydrogenation (Rh <sub>1</sub> )	99% 1-hexene conversion and 93.2% desired amine selectivity with linear to branched ratio of 1.1	23
5	Pd-PMA/ZrO <sub>2</sub>	C–C coupling (Pd <sub>1</sub> ) + hydrogenation (Pd <sub>1</sub> )	100% conversion and 99% selectivity for 2-aminobiphenyl	24
6	ADD–Fe–Al	Epoxidation (Fe sites) + cycloaddition (Al sites)	Around 97% styrene conversion and around 91% styrene carbonate selectivity	25
7	Rh <sub>1</sub> /CeO <sub>2</sub>	Water-gas shift (Rh <sub>1</sub> ) + hydroformylation (Rh <sub>1</sub> )	79% styrene conversion and 98% aldehyde selectivity with n/iso ratio of 3.0	26
8	Rh/TiO <sub>2</sub>	Water-gas shift (Rh <sub>1</sub> ) + <i>in situ</i> H <sub>2</sub> O <sub>2</sub> generation + oxidation (Rh <sub>1</sub> )	Millimole level yields of methanol with selectivity > 99%	27

<sup>a</sup>The active sites responsible for certain catalytic process are noted in the parentheses if authors have referenced them in the literature.

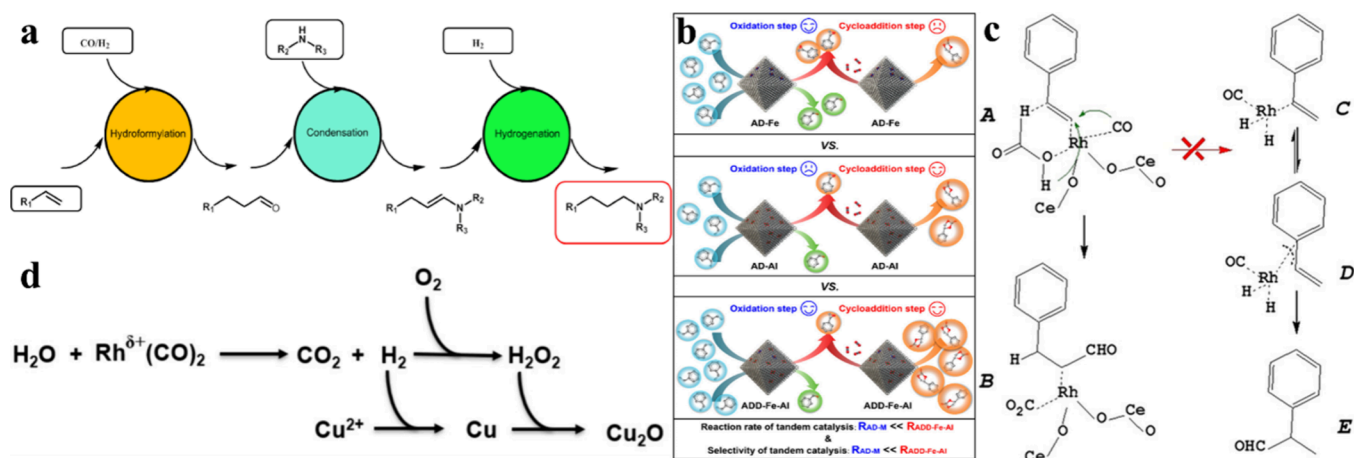


**Figure 4.** (a) General hydroaminomethylation reaction sequence. (b) Schematic illustration of the tandem catalytic strategy for improving the styrene oxidation rate and epoxidation selectivity in the presence of ADD–Fe–Al. (c) Proposed reaction route for the hydroformylation of styrene by coupling with LWGS. (d) Conversion mechanism of copper cations. Adapted with permission from (a) ref 23, (b) ref 25, (c) ref 26, and (d) ref 27. Copyright 2021 the authors of ref 23 under exclusive license to Elsevier, 2022 the authors of ref 25 under exclusive license to American Chemical Society, 2020 the authors of ref 26, and 2022 the authors of ref 27 under exclusive license to Wiley-VCH, respectively.

## 2. INTEGRATION OF SACs IN TANDEM CATALYSIS

### 2.1. Tandem Catalysis over Different/Identical Single Atom(s)

As single atoms are especially responsible for the heterogenization processes, mild hydrogenation/oxidation transformations, and maximum atom efficiency, single atoms themselves are suitable platforms to trigger tandem catalysis. For clear outline, we compile the tandem processes over single atoms according to the type of the involved catalytic reactions (Table 1).

**Isomerization in Tandem with Hydrosilylation.** As mentioned above, olefin hydrosilylation to produce industrially useful organosilane compounds is traditionally realized over molecular catalysts in homogeneous system, thereby facing low-efficiency recycling issues. As heterogeneous systems are inherently suitable for heterogenization of homogeneous processes, Sarma et al.<sup>20</sup> have investigated the catalytic behaviors over Rh and Ru single atoms under hydrosilylation conditions with  $\alpha$ -olefin as the substrate. Strikingly, Rh and Ru single atoms displayed exclusively selective for the anti-Markovnikov hydrosilylation of terminal olefins and double-bond isomerization, respectively, while the presence of metallic Rh could undesirably attribute to the enhanced rate of

isomerization over that of hydrosilylation. Therefore, the single-atom state of Rh species is the prerequisite for the highly selective  $\alpha$ -olefin hydrosilylation to the targeting terminal organosilane. Furthermore, combining the hydrosilylation-specific Rh single atoms with isomerization-specific Ru single atoms, the effective transformation of internal olefins, such as 2-octene, could be accomplished in one pot with an organosilane yield of 80% along with the valuable terminal-regioselectivity of as high as 92%. In contrast, it merely gave an organosilane yield of 33% over individual Rh single atoms due to the isomerization and hydrosilylation processes competing on the same active sites. Besides, the cooperation of two SACs can also allow the production of terminal organosilane compounds with high regioselectivity (>95%) from industrially relevant mixtures of terminal and internal olefins (Octene isomers mix and Neodene 8/9/10 isomers mix).

***In Situ* H<sub>2</sub> Generation in Tandem with Hydrogenation.** Liquid-phase chemical hydrogen storage materials, such as formic acid and ammonia borane, are proven to be suitable for H<sub>2</sub> storage techniques due to their high H<sub>2</sub> content and appropriate chemical stability considering the aspect of safety. Sun et al.<sup>21</sup> have prepared Rh single atoms encapsulated within silicalite-1 zeolite (Rh<sub>1</sub>@S-1) for efficient H<sub>2</sub> generation during the ammonia borane hydrolysis process with a H<sub>2</sub>

generation rate of  $432 \text{ mol}_{\text{H}_2} \text{ mol}_{\text{Rh}}^{-1} \text{ min}^{-1}$ . For comparison, the encapsulated Rh nanoparticles were also tested, yet only a  $\text{H}_2$  generation rate of  $195 \text{ mol}_{\text{H}_2} \text{ mol}_{\text{Rh}}^{-1} \text{ min}^{-1}$  was obtained, thus demonstrating the excellent  $\text{H}_2$  generation property over Rh single atoms.<sup>28</sup> Subsequently, based on the superior ability of  $\text{H}_2$  generation over SACs, the *in situ*  $\text{H}_2$  generation process was coupled with nitrobenzene hydrogenation and  $\text{Rh}_1@S-1$  exhibited >99% yield of amine products within 1.5 min. However, the conversion of nitrobenzene obviously dropped to as low as 5% even after 900 min when the ammonia borane was replaced by the conventional 1 bar of  $\text{H}_2$ , which unambiguously indicated the tandem hydrogenation protocol was much more effective than directly employing gaseous  $\text{H}_2$  as a hydrogen source. Likewise, single  $\text{CoN}_3$  sites in N-doped graphene-like carbon could also be employed in the tandem hydrogenation of nitrobenzene with  $\text{HCOOH}$  as the hydrogen donor, during which >99% nitrobenzene conversion and 96.3% aniline selectivity were attained.<sup>22</sup> After deliberately poisoning the  $\text{CoN}_3$  sites, the nitrobenzene conversion was dramatically decreased to 3.2% and therefore  $\text{CoN}_3$  sites were unveiled as the solely active site, which was a similar circumstance as that of the above  $\text{Rh}_1@S-1$  catalyst.

**Hydroaminomethylation.** Tandem hydroaminomethylation of olefins is an efficient and green route to produce chemical and pharmaceutical amines. The tandem hydroaminomethylation usually entails three consecutive processes, i.e., olefin hydroformylation to aldehydes, followed by *in situ* condensation with the other amine to form enamine, and finally the desired amine obtained via the hydrogenation of the internal  $\text{C}=\text{C}$  bond (Figure 4a). Generally, the homogeneously catalyzed hydroaminomethylation faces the dilemma of inconvenient separation of expensive noble metals and ligands. Therefore, Li et al.<sup>23</sup> have developed single-atom Rh supported on hydroxyapatite for tandem hydroaminomethylation, during which 99% 1-hexene conversion and 93.2% desired amine selectivity with a linear to branched ratio of 1.1 were successfully achieved. Among the three sequential processes, olefin hydroformylation was investigated as the rate-determining step and compared with Rh nanoparticles on other oxide supports, single-atom Rh demonstrated the highest hydroformylation activity, thereby ensuring outstanding hydroaminomethylation performance. Moreover, mechanism investigations also displayed that, apart from the spontaneous condensation process, the following hydrogenation step also occurred on the single  $\text{Rh}^+$  sites.

**C–C Coupling in Tandem with Hydrogenation.** Functionalized aminobiphenyl can be intentionally synthesized via Suzuki–Miyaura coupling and the sequential hydrogenation of nitrobiphenyl intermediates. In general, as the C–C coupling process is catalyzed by the homogeneous Pd complex, the inherent drawbacks of tedious separation and excess usage of organic solvents can readily be tackled by the employment of Pd single atoms. Patel et al.<sup>24</sup> prepared zirconia-supported phosphomolybdic acid stabilized Pd-single atom catalysts for the above tandem process, which gave almost 100% conversion and 99% aminobiphenyl selectivity. Hot filtration tests exhibited no obviously increased conversion after removal of the single-atom Pd catalysts at the interval of the reaction, confirming the heterogeneous nature of the as-prepared Pd single atoms. However, control experiments over Pd nanoparticles also gave similar catalytic results. This phenomenon possibly comes from Pd species leaching into the reaction

system, which should be carefully examined in future investigations.

**Epoxidation in Tandem with Cycloaddition.** Tandem oxidative carboxylation of olefins consists of epoxidation of olefins and sequential  $\text{CO}_2$  cycloaddition, which can be accomplished over atomically dispersed Fe–N–C and Al–O–C motifs, respectively. To improve the effectiveness of tandem oxidative carboxylation, Wang et al.<sup>25</sup> integrated dual Fe–Al sites on a carbon-based support, over which ~97% conversion and ~91% styrene carbonate selectivity were obtained taking styrene as the substrate. Based on the kinetic experiments of the disassembled process, Fe and Al sites were ascertained to be exclusively responsible for the oxidation of styrene and subsequent  $\text{CO}_2$  cycloaddition with epoxides, respectively (Figure 4b). Compared with the monometallic counterparts, the yield of targeted product over dual Fe–Al catalysts was at least 62% higher because the rapid consumption of styrene oxide intermediates could positively shift the equilibrium of the oxidation step, thus unequivocally exhibiting the cooperation of the sequential cycles in tandem processes, especially over the effective dual single-atom sites. Interestingly, the influence of distance between Fe/Al sites on the predicted catalytic performance was also studied via molecular dynamics simulations. The lengthened Fe/Al distance negatively prolonged the migration time and lowered the capture probability of the epoxide intermediate, leading to inferior catalytic performance. These preliminary results are inspiring for future investigations of the underlying influence of the distance between active single atoms on tandem catalytic performance because the mass transport of intermediates matters between sequential catalytic cycles.

**Water–Gas Shift in Tandem with Hydroformylation.** As discussed in the Introduction, single-atom catalysts are widely explored for the heterogenization of homogeneous catalysis, such as hydroformylation, to mitigate the energy input during separation process. However, the major challenge of improving the regioselectivity (*n*/*iso* ratio) over the heterogeneous one is typically tackled by maneuvering the steric hindrance around the Rh single atoms.<sup>29</sup> Surprisingly, a novel strategy to increase the regioselectivity can be achieved by *in situ* coupling hydroformylation with, for example, a water–gas shift process. In this case, Li et al.<sup>26</sup> have boosted the *n*/*iso* ratio to as high as 3.0 in the hydroformylation of styrene coupling with a low-temperature water–gas shift over  $\text{CeO}_2$  supported Rh SACs, while the conventional reaction conditions with CO and  $\text{H}_2$  as reactants only gave the *n*/*iso* ratio of 0.9. Furthermore, isopropanol and benzhydrol were chosen as *in situ* H donors to couple with hydroformylation as control experiments. In this regard, the *n*/*iso* ratios were comparable to that of hydroformylation in tandem with a low-temperature water–gas shift despite the lower activities, thereby convincingly verifying the predominant role of *in situ* H for the enhanced *n*/*iso* ratio, which might arise from the preferential coordination of intermediate formic acid with a  $\text{C}=\text{C}$  bond and leave the terminal end to be inserted with the carbonyl (Figure 4c). For comparison, the aldehyde products were prone to further hydrogenation to phenylpropanols over Rh nanoparticles, which corroborated the effectiveness of Rh single atoms for maintaining the high chemoselectivity of aldehyde products in hydroformylation.

**Water–Gas Shift in Tandem With *In Situ*  $\text{H}_2\text{O}_2$  Generation and Subsequent Oxidation.** Direct conversion of methane into value-added chemicals, such as methanol

Table 2. Tandem Catalysis over Single Atoms and Nanoparticles

Entry	Catalyst	Tandem path <sup>a</sup>	Key results	Ref
1	PdCu/Z-5	In-situ H <sub>2</sub> O <sub>2</sub> generation (PdO NPs) + oxidation (Cu <sub>1</sub> )	Oxygenates yield of 1178 mmol <sub>g<sub>pd</sub></sub> <sup>-1</sup> h <sup>-1</sup> with selectivity > 95%	32
2	Zn–N–C/Au@mSiO <sub>2</sub>	Epoxydation (Au NPs) + cycloaddition (Zn <sub>1</sub> )	93.2% styrene conversion and 99.7% styrene carbonate selectivity	33
3	PTF(Ni)/Cu	Electroreduction (PTF(Ni)) + dimerization (Cu NPs)	Faradaic efficiency of C <sub>2</sub> H <sub>4</sub> reaching 57.3% at –1.1 V versus RHE	34
4	CuO/Ni SAs	Electroreduction (Ni <sub>1</sub> ) + dimerization (CuO NPs)	Faradaic efficiency of C <sub>2</sub> H <sub>4</sub> reaching 54.1% at –0.892 V versus RHE	35

<sup>a</sup>The active sites responsible for certain catalytic process are noted in the parentheses if authors have referenced them in the literature.

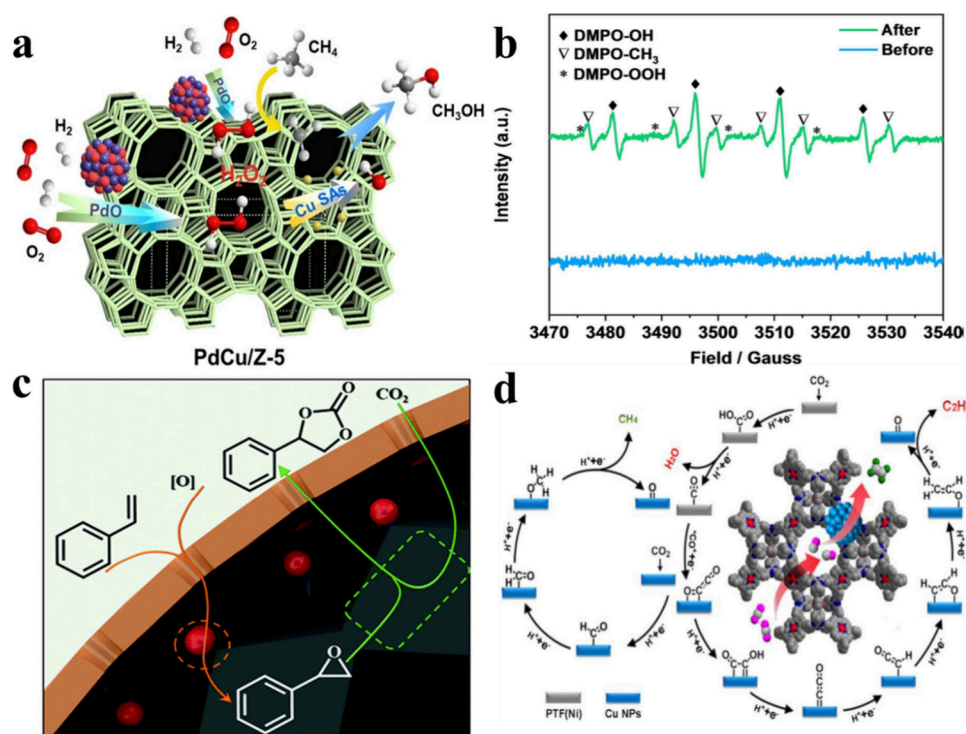


**Figure 5.** (a) Scheme of proposed reaction pathway for selective oxidation of CH<sub>4</sub> with O<sub>2</sub> and H<sub>2</sub> over PdCu/Z-5. (b) EPR trapping experiment with DMPO as the radical trapping agent over the PdCu/Z-5 catalyst. (c) Tandem transformation of styrene into styrene carbonate. (d) Possible reaction route for the formation of methane and ethylene. Adapted with permission from (a) and (b) ref 32, (c) ref 33, (d) ref 34. Copyright 2021 the authors of ref 33 under exclusive license to Royal Society of Chemistry, 2022 and 2021 the authors of ref 32 and ref 34 under exclusive license to Wiley-VCH, respectively.

under mild conditions, is considerably promising for industrial applications, yet it faces intractable challenges of activating inert C–H bonds in methane. Typically, a relatively expensive oxidant such as H<sub>2</sub>O<sub>2</sub> can adversely result in the overoxidation of the desired methanol to methyl peroxide and formic acid even if the thermodynamically stable C–H bond of CH<sub>4</sub> can be feasibly activated. Instead, moderate and inexpensive oxidants such as molecular O<sub>2</sub> are more feasible, considering the high methanol selectivity. Gu et al.<sup>27</sup> have integrated three sequential processes, i.e., water–gas shift reaction, *in situ* H<sub>2</sub>O<sub>2</sub> generation, and methane oxidation over atomically dispersed Rh supported on TiO<sub>2</sub> and as a result it reached a methanol yield of 1.3 mmol<sub>g<sub>cat</sub></sub><sup>-1</sup>h<sup>-1</sup> and activity of 68 mol<sub>mol<sub>Rh</sub></sub><sup>-1</sup>h<sup>-1</sup> with selectivity higher than 99%. Before the reaction, CO, O<sub>2</sub>, and CH<sub>4</sub> were all injected into the reactor as the initial reactants. The intermediate H<sub>2</sub>O<sub>2</sub> was synthesized *in situ* by the original O<sub>2</sub> and the generated H<sub>2</sub> from the water–gas shift reaction between CO and solvent H<sub>2</sub>O (Figure 4d). Afterward, methane could be steadily converted into methanol with the assistance of copper cations to maintain the necessary low-valence state of Rh species for methane adsorption and

suppress the formation of methyl peroxide byproduct. Rh single atoms were stated as the active sites for the water–gas shift reaction and methane oxidation, while the sites for H<sub>2</sub>O<sub>2</sub> generation remained obscure. For comparison, the obvious Rh–Rh scattering (2.32 Å) characteristic of Rh nanoparticles could be detected in EXAFS spectra after increasing the Rh loading content, which showed lower turnover frequency compared with the Rh SACs. This Rh SAC for methane oxidation may be promoted by the addition of Pd or Au species as the potential tandem catalysts because both Pd and Au are highly active for the synthesis of H<sub>2</sub>O<sub>2</sub> from molecular H<sub>2</sub> and O<sub>2</sub>.

## 2.2. Tandem Catalysis over Single Atoms and Nanoparticles

Although the sites with lone pairs of electrons, such as N, S elements and oxygen vacancies, responsible for anchoring single atoms are homogeneously distributed on supports.<sup>30,31</sup> These single-atom sites are still separated in nanoscale, often from several to tens of nanometers. Some catalytic processes that need multiple atoms in proximity are difficult to ignite or

Table 3. Tandem Catalysis over Single Atoms and the Support

Entry	Catalyst	Tandem path <sup>a</sup>	Key results	Ref
1	Pt/Ni <sub>3</sub> Fe	Hydrogenation (Pt <sub>1</sub> ) + hydrogenolysis (Ni <sub>3</sub> Fe)	99.0% 5-HMF conversion and 98.1% DMF yield	36
2	Pt/Co <sub>2</sub> AlO <sub>4</sub>	Hydrogenation (Pt <sub>1</sub> ) + hydrogenolysis (Co <sub>2</sub> AlO <sub>4</sub> )	99.0% 5-HMF conversion and 99% DMF selectivity	37
3	Pd/Au/TiO <sub>2</sub>	In-situ H <sub>2</sub> O <sub>2</sub> generation (Pd <sub>1</sub> Au NPs) + oxidation (TiO <sub>2</sub> )	Around 45% 2-propanol conversion	38
4	Ir <sub>1</sub> -Cu <sub>3</sub> N/ Cu <sub>2</sub> O	Water dissociation (Ir <sub>1</sub> ) + electroreduction (Cu <sub>3</sub> N/Cu <sub>2</sub> O)	Faradaic efficiency of CH <sub>4</sub> reaching 75% at -1.3 V versus RHE	39
5	Cr <sub>1</sub> /CoSe <sub>2</sub>	OER (CoSe <sub>2</sub> ) + oxidation (Cr <sub>1</sub> )	88% styrene conversion and 95% benzaldehyde selectivity under a potential of 1.6 V <sub>Ag/AgCl</sub>	40
6	In <sub>2</sub> O <sub>3</sub> /Cu-O <sub>3</sub>	CO <sub>2</sub> RR (In <sub>2</sub> O <sub>3</sub> ) + C-C coupling (Cu-O <sub>3</sub> )	Ethanol yield rate of 20.7 mmol g <sup>-1</sup> h <sup>-1</sup> with a high selectivity of 85.8% under visible-light irradiation	41

<sup>a</sup>The active sites responsible for certain catalytic process are noted in the parentheses if authors have referenced them in the literature.

occur with high efficiency just over SACs. With this regard, it is useful to couple nanoparticles with single atoms, during which both single atoms and nanoparticles take their responsibilities and fulfill the overall catalytic transformations (Table 2).

**In Situ H<sub>2</sub>O<sub>2</sub> Generation in Tandem with Oxidation.** Methane oxidation with the *in situ* H<sub>2</sub>O<sub>2</sub> generated from molecular H<sub>2</sub> and O<sub>2</sub> could also be transformed over the ZSM-5 supported PdCu bimetallic catalyst (PdCu/Z-5), where Pd and Cu species exist in the form of PdO nanoparticles and Cu single atoms, respectively.<sup>32</sup> The specific oxygenate (including CH<sub>3</sub>OH, CH<sub>3</sub>OOH, and HCOOH) yield over PdCu/Z-5 was 1178 mmol<sub>Pd</sub><sup>-1</sup>h<sup>-1</sup> along with 95% oxygenates selectivity. Nevertheless, if only methanol was considered as the criteria, the methanol yield was around 700 mmol<sub>Pd</sub><sup>-1</sup>h<sup>-1</sup>. Control experiments and mechanism studies clearly revealed that PdO nanoparticles were in charge of the *in situ* generation of H<sub>2</sub>O<sub>2</sub> from molecular H<sub>2</sub> and O<sub>2</sub> (Figure 5a), which probably resulted in the finally observed higher methanol yield compared with ref 27 over just Rh SACs. With regard to the subsequent methane oxidation process, Cu single atoms could accelerate the H<sub>2</sub>O<sub>2</sub> decomposition via the formation of hydroxyl radicals (·OH) instead of the undesired ·OOH radicals and then rendered the homolytic cleavage of CH<sub>4</sub> by ·OH to methyl radicals (·CH<sub>3</sub>), which were directly evidenced by the occurrence of peaks ascribed to ·OH and ·CH<sub>3</sub> species in the electron paramagnetic resonance spectra with 5,5-dimethyl-1-pyrroline-*N*-oxide (DMPO) as a radical scavenger (Figure 5b). For comparison, other ZSM-5 supported Pd-based catalysts (Pd-M/Z-5, M = Au, Fe, Co, Ni) were also systematically tested but exhibited either lower oxygenate yield or selectivity, thereby confirming the efficiency of the PdCu/Z-5 catalyst for this tandem process.

**Epoxidation in Tandem with Cycloaddition.** Apart from the above-mentioned dual Fe-Al sites, the tandem reaction of epoxidation of styrene and sequential cycloaddition with CO<sub>2</sub> as a coupling reagent can also be effectively realized over spatially compartmented Au nanoparticles and Zn single atoms, where Zn single atoms are uniformly distributed on the inner nitrogen-doped carbon shell, while Au nanoparticles are evenly confined between the inner shell and the outer SiO<sub>2</sub> protective shell for enhanced recyclability (Figure 5c).<sup>33</sup> The compartmented configuration ensured the efficient relay mode of the tandem process, during which Au nanoparticles were first accountable for the epoxidation of styrene and then the as-obtained intermediates transferred onto the Zn single-atom sites acting as Lewis acid like the above atomically dispersed Al sites for further cycloaddition with CO<sub>2</sub> to produce the aiming styrene carbonate. Under almost comparable reaction con-

ditions, this linkage of Au nanoparticles and Zn single atoms afforded 93.2% conversion and 99.7% styrene carbonate selectivity, which showed almost identical performance with that over dual Fe-Al sites in ref 25. Further control experiments over single catalytic sites (either Au nanoparticles or Zn single atoms) resulted in the benzaldehyde byproduct, thus validating the indispensability to couple the dual active sites.

#### Electroreduction in Tandem with Dimerization.

Electroreduction reaction of CO<sub>2</sub> (CO<sub>2</sub> RR) into valuable chemicals and carbon-based fuels offers an environmental-friendly technology to eliminate the atmospheric CO<sub>2</sub> and achieve the cyclic utilization of carbon resources. However, the deeper reduction of CO<sub>2</sub> into higher-value C<sub>2+</sub> products, such as C<sub>2</sub>H<sub>4</sub> is highly desirable but remains arduously challenging due to the involving multielectron transfer and sluggish C-C coupling dimerization steps. Therefore, in order to improve the catalytic efficiency and narrow down the product distribution in CO<sub>2</sub> RR, Meng et al.<sup>34</sup> developed tandem strategy to uniformly dispersed Cu nanoparticles on the atomically isolated nickel-nitrogen sites anchored on the porphyrinic triazine framework (PTF(Ni)/Cu), where PTF(Ni) could efficiently transform CO<sub>2</sub> to CO with high concentration, which ensured the subsequently high coverage over Cu sites for the sequential C-C coupling dimerization to C<sub>2</sub>H<sub>4</sub> instead of the formation of CH<sub>4</sub> (Figure 5d). The as-synthesized PTF(Ni)/Cu could produce C<sub>2</sub>H<sub>4</sub> with Faradaic efficiency as high as 57.3% at -1.1 V versus the reversible hydrogen electrode (RHE). For comparison, Cu nanoparticles supported on PTF without the addition of Ni species were also prepared, over which it merely obtained 9.6% C<sub>2</sub>H<sub>4</sub> selectivity, up to 6 times lower than that over PTF(Ni)/Cu. Furthermore, control experiments and density functional theory calculations affirmed that the CO-enriched local environment on the Cu sites generated from the nearby PTF(Ni) sites significantly led to the increased probability of C-C coupling and thus the single PTF(Ni) sites greatly embellishing the whole tandem process. Likewise, Zhang et al.<sup>35</sup> also fabricated Ni single atoms and CuO nanoparticles supported onto nitrogen-doped carbon for CO<sub>2</sub> RR, in which 54.1% Faradaic efficiency of C<sub>2</sub>H<sub>4</sub> was attained at -0.892 V versus RHE. Control experiments maneuvered the Ni single-atom sites and CuO nanoparticle sites to be separated by ways of either physical mixing or layer-by-layer spraying. However, the pivotal CO generation and sequential CO transfer to Cu sites were undesirably hindered, thereby revealing the importance of the local vicinity between Ni single atoms and CuO nanoparticles for the efficient utilization of the determining CO intermediates.

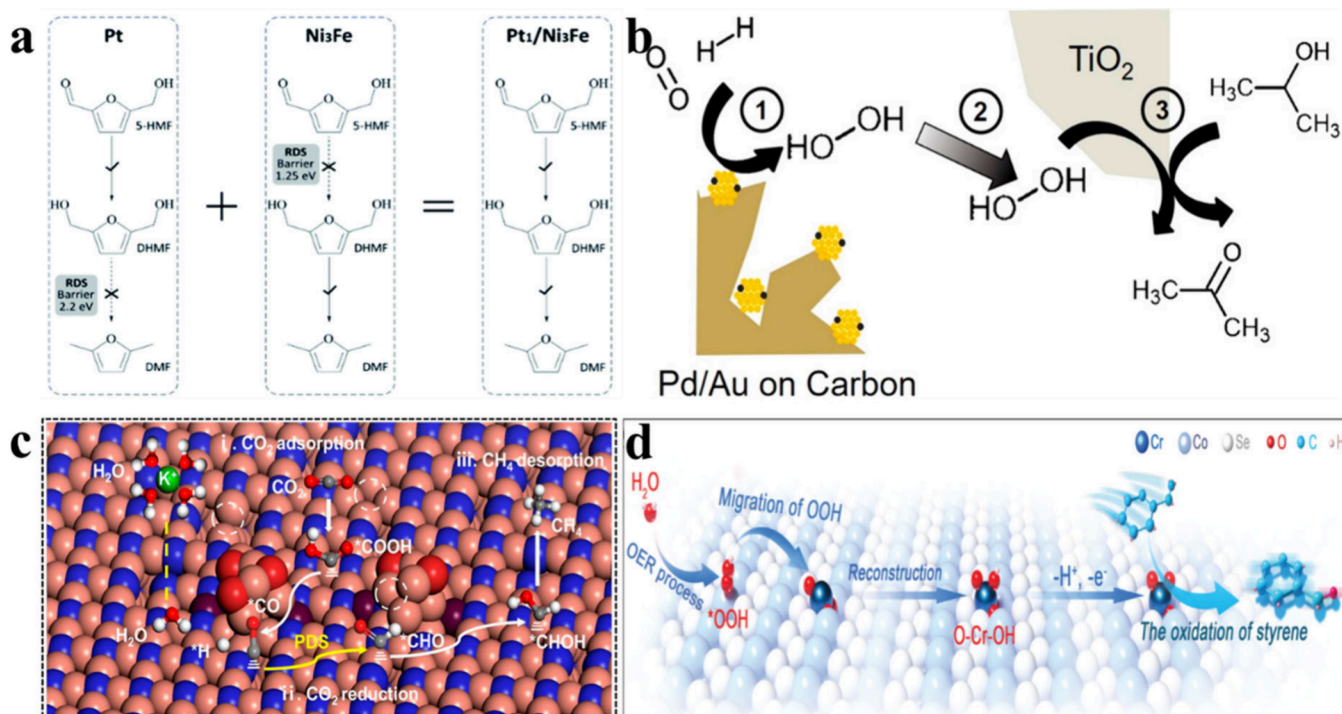


**Figure 6.** (a) Tandem mechanism on Pt/Ni<sub>3</sub>Fe, combining the catalytic performance of both Pt and Ni<sub>3</sub>Fe catalysts. (b) Reaction scheme demonstrating the formation of H<sub>2</sub>O<sub>2</sub> on Pd/Au nanoparticles immobilized on carbon (1), diffusion of H<sub>2</sub>O<sub>2</sub> to TiO<sub>2</sub> grains (2), and selective oxidation of 2-propanol on TiO<sub>2</sub> by H<sub>2</sub>O<sub>2</sub> (3). (c) Proposed reaction mechanism for the CO<sub>2</sub> RR to CH<sub>4</sub> on Ir<sub>1</sub>-Cu<sub>3</sub>N/Cu<sub>2</sub>O. The hollow white circles represent N or O vacancies. Green, K; brick red, Cu; purple, Ir; blue, N; red, O; gray, C; and white, H. (d) Schematic description of tandem path involving OER and styrene oxidation. Adapted with permission from (a) ref 36, (b) ref 38, (c) ref 39, and (d) ref 40. Copyright 2021 the authors of ref 36 under exclusive license to Royal Society of Chemistry, 2020 and 2022 the authors of ref 38 and ref 39 under exclusive license to American Chemical Society and 2022 the authors of ref 40 under exclusive license to Wiley-VCH, respectively.

### 2.3. Tandem Catalysis over Single Atoms and the Support

The above catalysts are constructed by single atoms/nanoparticles supported on crystalline oxide or amorphous carbon materials, which serve as the support of catalysts and almost show no activity for the catalytic cycles. However, in many cases, the significant properties of the supports, such as acidity and oxygen vacancies, are indispensable for some acid-catalyzed and oxidation processes. Therefore, it is prospective to integrate single atoms onto these supports with specific sites to cooperatively assemble tandem catalysts (Table 3).

#### Hydrogenation in Tandem with Hydrogenolysis.

Upgrading renewable biomass compounds to value-added chemicals is a promising strategy to mitigate the over-dependence on fossil fuels wherein 2,5-dimethylfuran (DMF) is regarded as an essential biomass-derived platform chemical for pharmaceutical industries. Accordingly, transformation of 5-hydroxymethylfurfural (5-HMF) to DMF via the hydrodeoxygenation reaction, which is the tandem process of hydrogenation and hydrogenolysis, is a promising but challenging approach due to the complexity of the reaction pathways, in parallel with the first step of preferable C=O hydrogenation, furan ring hydrogenation, and ring-opening side reactions. As discussed in the Introduction, single-atom catalysts are beneficial for polar C=O bond hydrogenation and thus are theoretically appropriate for the hydrodeoxygenation of 5-HMF to DMF. Therefore, Meng et al.<sup>36</sup> have devised Pt single atoms supported on intermetallic Ni<sub>3</sub>Fe, where Pt single atoms accounted for C=O hydrogenation and the Ni<sub>3</sub>Fe interface facilitated sequential C–OH bond rupture (Figure 6a), thus delivering a high catalytic performance with

99.0% 5-HMF conversion along with 98.1% DMF yield in 90 min at a low reaction temperature of 160 °C. Control experiments with Pt nanoparticles instead of Pt single atoms were carried out and merely gave 51.1% DMF yield after 120 min of reaction due to the inferior activity and the occurrence of above-mentioned side reactions, which illustrated the necessity of involving Pt single-atom sites. Additionally, Wang et al.<sup>37</sup> synthesized Pt single atoms anchored onto the Co<sub>2</sub>AlO<sub>4</sub> support, over which 99% 5-HMF conversion and 99% DMF selectivity were accomplished in 160 min at the reaction temperature of 180 °C. In this regard, the Brønsted acid sites (Co–O(H)–Al sites) adjacent to Pt single atoms were in charge of the C–OH bond cleavage. Similarly, the existence of PtO nanoparticles was also detrimental to the DMF selectivity, with only 28% DMF selectivity but 68% intermediate 5-methylfurfuryl alcohol selectivity under identical conditions, presumably resulting from the inhibition of activating the furan ring.

#### In Situ H<sub>2</sub>O<sub>2</sub> Generation in Tandem with Oxidation.

With regard to the selective oxidation reaction, Au nanoparticles supported on TiO<sub>2</sub> display remarkable catalytic performance even through the initial *in situ* H<sub>2</sub>O<sub>2</sub> generation process from molecular H<sub>2</sub> and O<sub>2</sub>. Despite the highly active Au nanoparticles for O<sub>2</sub> activation, the sluggish H<sub>2</sub> dissociation over the Au/TiO<sub>2</sub> interface may limit the whole tandem process. Therefore, Wrasman et al.<sup>38</sup> constructed Pd single atoms adhered onto Au nanoparticles (Pd/Au), where H<sub>2</sub> dissociation and O<sub>2</sub> activation producing H<sub>2</sub>O<sub>2</sub> took place over Pd single atoms and Au nanoparticles, respectively. Afterward, individual Au nanoparticles or composite Pd/Au was



supported on TiO<sub>2</sub> supports and physically mixed with TiO<sub>2</sub> for the selective oxidation of 2-propanol to acetone under hydro-oxidation conditions. Under identical reaction conditions, the physical mixed Au/TiO<sub>2</sub>(I)+TiO<sub>2</sub>(II) showed only around 25% 2-propanol conversion, while Pd/Au/TiO<sub>2</sub>(I)+TiO<sub>2</sub>(II) could offer roughly twice the activity because Pd single atoms were more advantageous for H<sub>2</sub> dissociation compared with the Au/TiO<sub>2</sub> interface. Therein, Pd/Au collectively worked for the *in situ* H<sub>2</sub>O<sub>2</sub> generation, which possibly transferred to both TiO<sub>2</sub>(I) supports and extra added TiO<sub>2</sub>(II) grains for subsequent propanol oxidation. To test this mechanism, inert carbon was also employed to support the active sites and remained physically mixed with TiO<sub>2</sub>(II). Strikingly, the Pd/Au nanoparticles supported on carbon were still able to effectively oxidize 2-propanol to acetone with approximately 25% conversion, while, for comparison, the individual Au nanoparticles were barely active. Those findings unequivocally confirmed that the *in situ* generated H<sub>2</sub>O<sub>2</sub> can diffuse from the Pd/Au sites to the neighboring TiO<sub>2</sub>(II) grains for the final 2-propanol oxidation to acetone (Figure 6b).

#### Water Dissociation in Tandem with Electroreduction.

Direct electrocatalytic conversion of CO<sub>2</sub> to CH<sub>4</sub> using water as a medium is regarded as a promising waste utilization approach. Nonetheless, the potential-determining step in this process, i.e., the intermediate \*CO combining with H<sup>+</sup> to form \*CHO, is considerably dependent on the inherent H<sup>+</sup> production and transformation properties of the catalysts. Therefore, a plausible tactic is to integrate highly active sites of water dissociation within the CO<sub>2</sub> methanation system. To this end, Chen et al.<sup>39</sup> presented a novel tandem catalyst composed of Ir single atoms doped on hybrid Cu<sub>3</sub>N/Cu<sub>2</sub>O to afford a high Faradaic efficiency of 75% for CH<sub>4</sub> at -1.3 V versus RHE. The *in situ* characterization and theoretical calculation results unraveled that Ir single atoms could facilitate the nucleophilic attack of water to form H<sup>+</sup> via promoting the absorption of -OH species and then motivated the protonation of the adsorbed \*CO<sub>2</sub> to \*COOH intermediate, which gave rise to rapid formation of \*CHO over the Ir<sub>1</sub>-Cu<sub>3</sub>N/Cu<sub>2</sub>O interface (Figure 6c). In contrast, if conducted over pure Cu<sub>3</sub>N, H<sub>2</sub>O molecule directly bound with the \*CO<sub>2</sub> intermediate and were difficult to further dissociate to H<sup>+</sup>, thus lowering the CH<sub>4</sub> Faradaic efficiency to less than 35%.

**Oxygen Evolution Reaction in Tandem with Oxidation.** Electrocatalytic oxidation of organic molecules with water as the oxygen source instead of exogenous oxidizing reagents is a promising but tricky strategy to produce value-added chemicals due to the compromise of catalytic efficiency resulting from the competitive oxygen evolution reaction (OER) process. To take advantage of the oxidizing intermediates from the OER process, Dang et al.<sup>40</sup> devised the oxidation of styrene process in tandem with the OER process over CoSe<sub>2</sub> supported Cr single atoms (Cr<sub>1</sub>/CoSe<sub>2</sub>). Therein, Co sites on the CoSe<sub>2</sub> support and Cr single atoms were accountable for the OER and styrene oxidation to benzaldehyde, respectively. Control experiments have suggested that Cr<sub>1</sub>/CoSe<sub>2</sub> presented a higher total current density from 1.4 to 2.0 V<sub>Ag/AgCl</sub> compared with a pure CoSe<sub>2</sub> support, where barely any benzaldehyde products could be detected. Thus, the depletion of oxidizing intermediates (\*OOH) could positively promote the equilibrium of the OER process, which led to excellent catalytic performance of 95% selectivity to benzaldehyde and a high conversion of styrene at 88% under a

potential of 1.6 V<sub>Ag/AgCl</sub>. Afterward, isotopic tracing, *in situ* Raman spectra together with theoretical calculations comprehensively verified that the \*OOH intermediates generated over CoSe<sub>2</sub> effectively linked the OER and oxidation process by transferring from the Co sites on CoSe<sub>2</sub> support to the Cr single atoms (Figure 6d). This efficient migration of \*OOH intermediates could then greatly accelerate the dynamics of styrene oxidation occurring over the reconstructed O-Cr-OH sites.

**CO<sub>2</sub> Reduction Reaction in Tandem with C-C Coupling.** Apart from the above CO<sub>2</sub> reduction into value-added C<sub>2+</sub> products under electrocatalysis conditions as reported in refs 34 and 35, artificial photosynthesis can also contribute to this process to produce the C<sub>2</sub> liquid fuels, such as ethanol. However, this photocatalysis process still suffers from the demanding nature of multi-electron-proton transfers and intractable C-C couplings. To improve the ethanol yield rate, Gong et al.<sup>41</sup> have created 3-coordinated Cu single atoms supported on the In<sub>2</sub>O<sub>3</sub> support (In<sub>2</sub>O<sub>3</sub>/Cu-O<sub>3</sub>), where the Cu-O-In sites mostly transformed CO<sub>2</sub> into high-coverage \*CO intermediates and the Cu single atoms promoted the crucial C-C coupling. Consequently, In<sub>2</sub>O<sub>3</sub>/Cu-O<sub>3</sub> remarkably showed an ethanol yield rate of 20.7 mmol g<sup>-1</sup> h<sup>-1</sup> with a high selectivity of 85.8% under visible-light irradiation. The 3-coordinated Cu single atoms were tested especially necessary for this tandem process in two controlled experiments: first, unmodified In<sub>2</sub>O<sub>3</sub> almost gave undetectable C<sub>2</sub> products and most products were just C<sub>1</sub> molecules such as CO and CH<sub>4</sub>; second, the modulated 4-coordinated In<sub>2</sub>O<sub>3</sub>/Cu-O<sub>4</sub> was also inactive for ethanol production. Furthermore, theoretical calculations compared the formation energies of three possible C-C coupling processes, i.e., conventional \*CO dimerization (OC-CO coupling), coupling of \*CO and \*COH (OC-COH coupling), and coupling of \*CO and \*CH<sub>3</sub> (OC-CH<sub>3</sub> coupling) over Cu single-atom sites. As a result, OC-COH coupling was the most favorable C-C coupling among these three processes. However, the single-atom sites are widely known for the difficulty in boosting the C-C coupling process. The unexpected mechanism in this work may result from the proximity between the Cu-O-In sites and the following Cu single-atom sites. Further investigations are highly expected over the tandem system with single-atom active sites in such local vicinity for the promotion of C-C coupling processes.

### 3. CONCLUSIONS AND PERSPECTIVES

In summary, compared with conducting sequential reactions in different reactors or batches, the tandem catalysis processes in one pot realize the “1 + 1 > 2” mode because the separate active sites in the proximity can greatly boost the efficiency of mass transport where the products from the first reaction cycle can directly transfer to the second reaction cycle as the reactants. However, the “tandem catalysis” concept is sometimes liable to be muddled with other concepts, such as “synergy” or “domino/cascade catalysis”. The prerequisites to ascertain “tandem catalysis” mainly lie in that (1) tandem catalysis processes involve the coupling of sequential catalytic cycles and (2) these catalytic cycles must proceed with different mechanisms. Although the SACs have been applied and proven effectful in various heterogeneous catalysis processes, SACs may not be the solutions for efficient catalytic transformations requiring multiatoms in proximity. Therefore, it is reasonable to integrate single-atom sites with other single-atom sites, nanoparticles, and supports. Therein, SACs are still

responsible for the characteristic (1) high metal-normalized activity in, such as, *in situ* H<sub>2</sub> generation and oxidative processes, (2) selective hydrogenation of specific polar bonds, such as C=O, and (3) inherent advantages in bridging homogeneous and heterogeneous catalysis, such as in hydroformylation and hydrosilylation. Moreover, with regard to the catalytic processes that need abundant acid sites or oxygen vacancies that cannot be provided by merely single atoms or nanoparticles, the supports bearing the above sites (e.g., H-type zeolites for acid sites and reducible oxides for oxygen vacancies) should play an indispensable role after depositing single atoms for tandem catalysis.

However, there still exist some issues when we integrate single-atom catalysts into tandem processes. First, it is not rigorous to make conclusions that the single atoms are the real active sites since the samples have not been systematically characterized via the combination of aberration-corrected scanning transmission electron microscopy, X-ray absorption spectroscopy, and CO diffuse reflectance infrared Fourier transform spectroscopy.<sup>42</sup> If not thoroughly investigated, nanoclusters may coexist with single atoms and thereby can considerably obscure the real catalytic mechanism in the tandem process. Second, after integrating single atoms, the distinct catalytic performances should be judiciously compared with those over nanoclusters or nanoparticles.<sup>43–45</sup> On top of that comparison, it is then reasonable to state the necessity of single-atom sites in the specific tandem process. Third, the responsibility of each active site for the individual reaction process is still vague sometimes, and therefore, it is imperative to figure out exactly the catalytic role of each site through the meticulously designed control experiments and theoretical calculations. Additionally, tandem active sites coupled in proximity can possibly trigger different reaction mechanisms, in comparison with separate catalytic processes. In this case, *in situ* spectroscopy experiments should be conducted to examine the adsorbed intermediates and possible transformation of coordination states of the active sites, which potentially provide deeper insights into tandem catalysis and improve the rational design of tandem catalytic processes in turn.

Apart from the above-reported tandem processes in the literature, there are still some challenging subjects to be tackled via the promising tandem strategy:

- (1) The alkene hydroformylation can be tentatively coupled with reverse water–gas shift (RWGS) process with CO<sub>2</sub> and H<sub>2</sub> as reactants to produce CO instead of the direct usage of syngas. Generally, this tandem process is carried out over Ru<sup>46</sup> or Rh-based<sup>47</sup> homogeneous catalysts. Further heterogenization of alkene hydroformylation with CO<sub>2</sub>/H<sub>2</sub> has just been applied over Au-based catalysts whereas the consequences suffer from fairly low activity,<sup>48</sup> probably due to the thermodynamical mismatch between the RWGS and the hydroformylation process. In theory, the thermodynamically mismatched reactions often render obstacles for realizing tandem processes unless highly active catalysts are discovered to mitigate the thermodynamical mismatch as far as possible. Therefore, in this case, if Rh SACs responsible for hydroformylation are integrated with other RWGS catalysts, for example, recent Fe–Pt/CeO<sub>2</sub>,<sup>49</sup> which exhibits a remarkable TOF<sub>Pt</sub> of 43,519 h<sup>-1</sup> with ~100% CO selectivity at a relatively low temperature of 350 °C, it may be plausible to achieve the effective RWGS-

hydroformylation tandem process. Besides, water–gas shift reaction has also been successfully coupled with selective alkyne hydrogenation over  $\alpha$ -MoC catalysts<sup>50,51</sup> or integrated with CO hydrogenation,<sup>52</sup> known as Kölbl-Engelhardt synthesis for producing hydrocarbons over photothermal TiO<sub>2-x</sub>/Ni. Considering that Pt and Au single atoms are efficient for water–gas shift reaction,<sup>53,54</sup> it would be interesting to examine the catalytic performances of above tandem processes integrated with SACs.

- (2) The as-discussed catalysts mostly pertain to active metal species loaded onto the surface of supports, thus only considering the geometric and electronic effects.<sup>55</sup> Besides, the encapsulation effect is also an intriguing theme when the single-atom species are encapsulated within the porous structures such as zeolite and metal organic frameworks (MOFs)<sup>56</sup> because the inherent steric hindrance definitely influences the selective transformation of molecules with dynamic diameters similar to or smaller than the pore sizes of crystalline frameworks, known as shape-selectivity. Therefore, it is greatly interesting to encapsulate different single-atom sites and nanoparticles within porous materials for conducting tandem processes in a confined micro-environment. Moreover, as mentioned above, the crystalline porous materials can also offer abundant acid sites, such as H<sup>+</sup> as the Brønsted acid in H-type zeolites and metal nodes as the Lewis acid in MOFs, which can also cooperatively transform the low-value reactants to the desired products in one pot.
- (3) The reported single atoms are predominantly supported with other single-atom sites and nanoparticles in random distribution. Thus, it remains unclear to what extent the proximity between different sites is most suitable for the mass-transfer of intermediates in tandem processes. As references, the density of single atoms on supports can be controlled via adjusting the surface composition of supports and the synthetic methods.<sup>57</sup> In addition, the density of single atoms can be quantitatively measured based on the physical sorption, aberration-corrected scanning transmission electron microscopy and theoretical calculations. Therefore, this paradigm can be extrapolated to the investigation of the suitable proximity/distance between single-atom sites and other active sites in tandem catalysis for improved catalytic performances.

## ■ AUTHOR INFORMATION

### Corresponding Authors

**Botao Qiao** – CAS Key Laboratory of Science and Technology on Applied Catalysis and State Key Laboratory of Catalysis, Dalian Institute of Chemical Physics, Chinese Academy of Sciences, 116023 Dalian, China; [orcid.org/0000-0001-6351-455X](https://orcid.org/0000-0001-6351-455X); Email: [bqiao@dicp.ac.cn](mailto:bqiao@dicp.ac.cn)

**Tao Zhang** – CAS Key Laboratory of Science and Technology on Applied Catalysis, Dalian Institute of Chemical Physics, Chinese Academy of Sciences, 116023 Dalian, China; [orcid.org/0000-0001-9470-7215](https://orcid.org/0000-0001-9470-7215); Email: [taozhang@dicp.ac.cn](mailto:taozhang@dicp.ac.cn)

## Author

Cun Liu – CAS Key Laboratory of Science and Technology on Applied Catalysis, Dalian Institute of Chemical Physics, Chinese Academy of Sciences, 116023 Dalian, China

Complete contact information is available at:  
<https://pubs.acs.org/10.1021/jacsau.4c00784>

## Author Contributions

CRedit: Cun Liu data curation, formal analysis, investigation, writing - original draft, writing - review & editing; Botao Qiao conceptualization, funding acquisition, methodology, project administration, supervision, writing - review & editing; Tao Zhang conceptualization, funding acquisition, project administration, supervision, writing - review & editing.

## Notes

The authors declare no competing financial interest.

## ACKNOWLEDGMENTS

This work was financially supported by National Key Research and Development Program of China (2021YFA1500503), National Natural Science Foundation of China (21961142006, 22388102, U23A20110, 22402192), and CAS Project for Young Scientists in Basic Research (YSBR-022).

## REFERENCES

- (1) Lohr, T. L.; Marks, T. J. Orthogonal Tandem Catalysis. *Nat. Chem.* **2015**, *7* (6), 477–482.
- (2) Garg, S.; Xie, Z.; Chen, J. G. Tandem Reactors and Reactions for CO<sub>2</sub> Conversion. *Nat. Chem. Eng.* **2024**, *1* (2), 139–148.
- (3) Patra, S.; Maity, N. Recent Advances in (Hetero)Dimetallic Systems towards Tandem Catalysis. *Coordin. Chem. Rev.* **2021**, *434*, No. 213803.
- (4) Wasilke, J.-C.; Obrey, S. J.; Baker, R. T.; Bazan, G. C. Concurrent Tandem Catalysis. *Chem. Rev.* **2005**, *105* (3), 1001–1020.
- (5) Rodenas, T.; Prieto, G. Solid Single-Atom Catalysts in Tandem Catalysis: Lookout, Opportunities and Challenges. *ChemCatChem* **2022**, *14* (23), No. e202201058.
- (6) Shi, J. On the Synergetic Catalytic Effect in Heterogeneous Nanocomposite Catalysts. *Chem. Rev.* **2013**, *113* (3), 2139–2181.
- (7) Tang, Y.; Wei, Y.; Wang, Z.; Zhang, S.; Li, Y.; Nguyen, L.; Li, Y.; Zhou, Y.; Shen, W.; Tao, F. F.; Hu, P. Synergy of Single-Atom Ni<sub>1</sub> and Ru<sub>1</sub> Sites on CeO<sub>2</sub> for Dry Reforming of CH<sub>4</sub>. *J. Am. Chem. Soc.* **2019**, *141* (18), 7283–7293.
- (8) Ramasamy, B.; Ghosh, P. The Developing Concept of Bifunctional Catalysis with Transition Metal N-Heterocyclic Carbene Complexes. *Eur. J. Inorg. Chem.* **2016**, *2016* (10), 1448–1465.
- (9) Ro, I.; Qi, J.; Lee, S.; Xu, M.; Yan, X.; Xie, Z.; Zakem, G.; Morales, A.; Chen, J. G.; Pan, X.; Vlachos, D. G.; Caratzoulas, S.; Christopher, P. Bifunctional Hydroformylation on Heterogeneous Rh-WO<sub>x</sub> Pair Site Catalysts. *Nature* **2022**, *609* (7926), 287–292.
- (10) Fogg, D. E.; dos Santos, E. N. Tandem Catalysis: A Taxonomy and Illustrative Review. *Coordin. Chem. Rev.* **2004**, *248* (21–24), 2365–2379.
- (11) Guo, Y.; Huang, Y.; Zeng, B.; Han, B.; AKRI, M.; Shi, M.; Zhao, Y.; Li, Q.; Su, Y.; Li, L.; Jiang, Q.; Cui, Y.-T.; Li, L.; Li, R.; Qiao, B.; Zhang, T. Photo-Thermo Semi-Hydrogenation of Acetylene on Pd<sub>1</sub>/TiO<sub>2</sub> Single-Atom Catalyst. *Nat. Commun.* **2022**, *13* (1), 2648.
- (12) Zhang, J.; Wang, M.; Gao, Z.; Qin, X.; Xu, Y.; Wang, Z.; Zhou, W.; Ma, D. Importance of Species Heterogeneity in Supported Metal Catalysts. *J. Am. Chem. Soc.* **2022**, *144* (11), 5108–5115.
- (13) Qiao, B.; Wang, A.; Yang, X.; Allard, L. F.; Jiang, Z.; Cui, Y.; Liu, J.; Li, J.; Zhang, T. Single-Atom Catalysis of CO Oxidation Using Pt<sub>1</sub>/FeO<sub>x</sub>. *Nat. Chem.* **2011**, *3* (8), 634–641.
- (14) Yan, H.; Cheng, H.; Yi, H.; Lin, Y.; Yao, T.; Wang, C.; Li, J.; Wei, S.; Lu, J. Single-Atom Pd<sub>1</sub>/Graphene Catalyst Achieved by Atomic Layer Deposition: Remarkable Performance in Selective Hydrogenation of 1,3-Butadiene. *J. Am. Chem. Soc.* **2015**, *137* (33), 10484–10487.
- (15) Deng, X.; Qin, B.; Liu, R.; Qin, X.; Dai, W.; Wu, G.; Guan, N.; Ma, D.; Li, L. Zeolite-Encaged Isolated Platinum Ions Enable Heterolytic Dihydrogen Activation and Selective Hydrogenations. *J. Am. Chem. Soc.* **2021**, *143* (49), 20898–20906.
- (16) Shi, Y.; Zhou, Y.; Lou, Y.; Chen, Z.; Xiong, H.; Zhu, Y. Homogeneity of Supported Single-Atom Active Sites Boosting the Selective Catalytic Transformations. *Adv. Sci.* **2022**, *9* (24), 2201520.
- (17) Chen, F.; Jiang, X.; Zhang, L.; Lang, R.; Qiao, B. Single-Atom Catalysis: Bridging the Homo- and Heterogeneous Catalysis. *Chin. J. Catal.* **2018**, *39* (5), 893–898.
- (18) Chen, Z.; Liu, J.; Koh, M. J.; Loh, K. P. Single-Atom Catalysis: From Simple Reactions to the Synthesis of Complex Molecules. *Adv. Mater.* **2022**, *34* (25), 2103882.
- (19) Liang, X.; Fu, N.; Yao, S.; Li, Z.; Li, Y. The Progress and Outlook of Metal Single-Atom-Site Catalysis. *J. Am. Chem. Soc.* **2022**, *144* (40), 18155–18174.
- (20) Sarma, B. B.; Kim, J.; Amsler, J.; Agostini, G.; Weidenthaler, C.; Pfänder, N.; Arenal, R.; Concepción, P.; Plessow, P.; Studt, F.; Prieto, G. One-Pot Cooperation of Single-Atom Rh and Ru Solid Catalysts for a Selective Tandem Olefin Isomerization-Hydrosilylation Process. *Angew. Chem., Int. Ed.* **2020**, *59* (14), 5806–5815.
- (21) Sun, Q.; Wang, N.; Zhang, T.; Bai, R.; Mayoral, A.; Zhang, P.; Zhang, Q.; Terasaki, O.; Yu, J. Zeolite-Encaged Single-Atom Rhodium Catalysts: Highly-Efficient Hydrogen Generation and Shape-Selective Tandem Hydrogenation of Nitroarenes. *Angew. Chem., Int. Ed.* **2019**, *58* (51), 18570–18576.
- (22) Zhang, F.; Li, J.; Liu, P.; Li, H.; Chen, S.; Li, Z.; Zan, W. Y.; Guo, J.; Zhang, X. M. Ultra-High Loading Single CoN<sub>3</sub> Sites in N-Doped Graphene-like Carbon for Efficient Transfer Hydrogenation of Nitroaromatics. *J. Catal.* **2021**, *400*, 40–49.
- (23) Li, X.; Li, L.; Qin, T.; Gun, G.; Lin, T.; Zhong, L. Atomically Dispersed Rh on Hydroxyapatite as an Effective Catalyst for Tandem Hydroaminomethylation of Olefins. *Mol. Catal.* **2021**, *509* (June), No. 111671.
- (24) Patel, J. R.; Patel, A. U. Pd Single-Atom-Site Stabilized by Supported Phosphomolybdic Acid: Design, Characterizations and Tandem Suzuki–Miyaura Cross Coupling/Nitro Hydrogenation Reaction. *Nanoscale Adv.* **2022**, *4* (20), 4321–4334.
- (25) Wang, Y.; Tian, Z.; Yang, Q.; Tong, K.; Tang, X.; Zhang, N.; Zhou, J.; Zhang, L.; Zhang, Q.; Dai, S.; Lin, Y.; Lu, Z.; Chen, L. Atomically Dispersed Dual Metal Sites Boost the Efficiency of Olefins Epoxidation in Tandem with CO<sub>2</sub> Cycloaddition. *Nano Lett.* **2022**, *22* (20), 8381–8388.
- (26) Li, T.; Chen, F.; Lang, R.; Wang, H.; Su, Y.; Qiao, B.; Wang, A.; Zhang, T. Styrene Hydroformylation with In Situ Hydrogen: Regioselectivity Control by Coupling with the Low-Temperature Water–Gas Shift Reaction. *Angew. Chem., Int. Ed.* **2020**, *59* (19), 7430–7434.
- (27) Gu, F.; Qin, X.; Li, M.; Xu, Y.; Hong, S.; Ouyang, M.; Giannakakis, G.; Cao, S.; Peng, M.; Xie, J.; Wang, M.; Han, D.; Xiao, D.; Wang, X.; Wang, Z.; Ma, D. Selective Catalytic Oxidation of Methane to Methanol in Aqueous Medium over Copper Cations Promoted by Atomically Dispersed Rhodium on TiO<sub>2</sub>. *Angew. Chem., Int. Ed.* **2022**, *61* (18), No. e202201540.
- (28) Sun, Q.; Wang, N.; Xu, Q.; Yu, J. Nanopore-Supported Metal Nanocatalysts for Efficient Hydrogen Generation from Liquid-Phase Chemical Hydrogen Storage Materials. *Adv. Mater.* **2020**, *32*, 2001818.
- (29) Zhang, X.; Yan, T.; Hou, H.; Yin, J.; Wan, H.; Sun, X.; Zhang, Q.; Sun, F.; Wei, Y.; Dong, M.; Fan, W.; Wang, J.; Sun, Y.; Zhou, X.; Wu, K.; Yang, Y.; Li, Y.; Cao, Z. Regioselective Hydroformylation of Propene Catalysed by Rhodium-Zeolite. *Nature* **2024**, *629* (8012), 597–602.

- (30) Wei, S.; Li, A.; Liu, J. C.; Li, Z.; Chen, W.; Gong, Y.; Zhang, Q.; Cheong, W. C.; Wang, Y.; Zheng, L.; Xiao, H.; Chen, C.; Wang, D.; Peng, Q.; Gu, L.; Han, X.; Li, J.; Li, Y. Direct Observation of Noble Metal Nanoparticles Transforming to Thermally Stable Single Atoms. *Nat. Nanotechnol.* **2018**, *13* (9), 856–861.
- (31) Yang, J.; Qi, H.; Li, A.; Liu, X.; Yang, X.; Zhang, S.; Zhao, Q.; Jiang, Q.; Su, Y.; Zhang, L.; Li, J.-F.; Tian, Z.-Q.; Liu, W.; Wang, A.; Zhang, T. Potential-Driven Restructuring of Cu Single Atoms to Nanoparticles for Boosting the Electrochemical Reduction of Nitrate to Ammonia. *J. Am. Chem. Soc.* **2022**, *144* (27), 12062–12071.
- (32) Wu, B.; Lin, T.; Huang, M.; Li, S.; Li, J.; Yu, X.; Yang, R.; Sun, F.; Jiang, Z.; Sun, Y.; Zhong, L. Tandem Catalysis for Selective Oxidation of Methane to Oxygenates Using Oxygen over PdCu/Zeolite. *Angew. Chem., Int. Ed.* **2022**, *61* (24), No. e202204116.
- (33) Hou, Y.; Wang, X.; Guo, Y.; Zhang, X. Double-Shell Microcapsules with Spatially Arranged Au Nanoparticles and Single Zn Atoms for Tandem Synthesis of Cyclic Carbonates. *Nanoscale* **2021**, *13* (44), 18695–18701.
- (34) Meng, D.-L.; Zhang, M.-D.; Si, D.-H.; Mao, M.-J.; Hou, Y.; Huang, Y.-B.; Cao, R. Highly Selective Tandem Electroreduction of CO<sub>2</sub> to Ethylene over Atomically Isolated Nickel-Nitrogen Site/Copper Nanoparticle Catalysts. *Angew. Chem., Int. Ed.* **2021**, *60* (48), 25485–25492.
- (35) Zhang, Y.; Li, P.; Zhao, C.; Zhou, G.; Zhou, F.; Zhang, Q.; Su, C.; Wu, Y. Multicarbon Generation Factory: CuO/Ni Single Atoms Tandem Catalyst for Boosting the Productivity of CO<sub>2</sub> Electrocatalysis. *Sci. Bull.* **2022**, *67* (16), 1679–1687.
- (36) Meng, G.; Ji, K.; Zhang, W.; Kang, Y.; Wang, Y.; Zhang, P.; Wang, Y. G.; Li, J.; Cui, T.; Sun, X.; Tan, T.; Wang, D.; Li, Y. Tandem Catalyzing the Hydrodeoxygenation of 5-Hydroxymethylfurfural over a Ni<sub>3</sub>Fe Intermetallic Supported Pt Single-Atom Site Catalyst. *Chem. Sci.* **2021**, *12* (11), 4139–4146.
- (37) Wang, L.; Yang, Y.; Shi, Y.; Liu, W.; Tian, Z.; Zhang, X.; Zheng, L.; Hong, S.; Wei, M. Single-Atom Catalysts with Metal-Acid Synergistic Effect toward Hydrodeoxygenation Tandem Reactions. *Chem. Catal.* **2023**, *3* (1), 100483.
- (38) Wrasman, C. J.; Riscoe, A. R.; Lee, H.; Cargnello, M. Dilute Pd/Au Alloys Replace Au/TiO<sub>2</sub> Interface for Selective Oxidation Reactions. *ACS Catal.* **2020**, *10* (3), 1716–1720.
- (39) Chen, S.; Zhang, Z.; Jiang, W.; Zhang, S.; Zhu, J.; Wang, L.; Ou, H.; Zaman, S.; Tan, L.; Zhu, P.; Zhang, E.; Jiang, P.; Su, Y.; Wang, D.; Li, Y. Engineering Water Molecules Activation Center on Multisite Electrocatalysts for Enhanced CO<sub>2</sub> Methanation. *J. Am. Chem. Soc.* **2022**, *144* (28), 12807–12815.
- (40) Dang, K.; Dong, H.; Wang, L.; Jiang, M.; Jiang, S.; Sun, W.; Wang, D.; Tian, Y. Boosting Electrochemical Styrene Transformation via Tandem Water Oxidation over a Single-Atom Cr<sub>1</sub>/CoSe<sub>2</sub> Catalyst. *Adv. Mater.* **2022**, *34* (27), 2200302.
- (41) Gong, S.; Ni, B.; He, X.; Wang, J.; Jiang, K.; Wu, D.; Min, Y.; Li, H.; Chen, Z. Electronic Modulation of a Single-Atom-Based Tandem Catalyst Boosts CO<sub>2</sub> Photoreduction to Ethanol. *Energy Environ. Sci.* **2023**, *16* (12), 5956–5969.
- (42) Sarma, B. B.; Maurer, F.; Doronkin, D. E.; Grunwaldt, J.-D. Design of Single-Atom Catalysts and Tracking Their Fate Using *Operando* and Advanced X-Ray Spectroscopic Tools. *Chem. Rev.* **2023**, *123* (1), 379–444.
- (43) Guo, Y.; Wang, M.; Zhu, Q.; Xiao, D.; Ma, D. Ensemble Effect for Single-Atom, Small Cluster and Nanoparticle Catalysts. *Nat. Catal.* **2022**, *5* (9), 766–776.
- (44) Liu, L.; Corma, A. Metal Catalysts for Heterogeneous Catalysis: From Single Atoms to Nanoclusters and Nanoparticles. *Chem. Rev.* **2018**, *118* (10), 4981–5079.
- (45) Liu, L.; Meira, D. M.; Arenal, R.; Concepcion, P.; Puga, A. V.; Corma, A. Determination of the Evolution of Heterogeneous Single Metal Atoms and Nanoclusters under Reaction Conditions: Which Are the Working Catalytic Sites? *ACS Catal.* **2019**, *9* (12), 10626–10639.
- (46) Tominaga, K.; Sasaki, Y. Ruthenium Complex-Catalyzed Hydroformylation of Alkenes with Carbon Dioxide. *Catal. Commun.* **2000**, *1* (1–4), 1–3.
- (47) Ren, X.; Zheng, Z.; Zhang, L.; Wang, Z.; Xia, C.; Ding, K. Rhodium-Complex-Catalyzed Hydroformylation of Olefins with CO<sub>2</sub> and Hydrosilane. *Angew. Chem., Int. Ed.* **2017**, *56* (1), 310–313.
- (48) Ahlers, S. J.; Bentrup, U.; Linke, D.; Kondratenko, E. V. An Innovative Approach for Highly Selective Direct Conversion of CO<sub>2</sub> into Propanol Using C<sub>2</sub>H<sub>4</sub> and H<sub>2</sub>. *ChemSusChem* **2014**, *7* (9), 2631–2639.
- (49) Wang, H.; Bootharaju, M. S.; Kim, J. H.; Wang, Y.; Wang, K.; Zhao, M.; Zhang, R.; Xu, J.; Hyeon, T.; Wang, X.; Song, S.; Zhang, H. Synergistic Interactions of Neighboring Platinum and Iron Atoms Enhance Reverse Water–Gas Shift Reaction Performance. *J. Am. Chem. Soc.* **2023**, *145* (4), 2264–2270.
- (50) Huang, R.; Xia, M.; Zhang, Y.; Guan, C.; Wei, Y.; Jiang, Z.; Li, M.; Zhao, B.; Hou, X.; Wei, Y.; Chen, Q.; Hu, J.; Cui, X.; Yu, L.; Deng, D. Acetylene Hydrogenation to Ethylene by Water at Low Temperature on a Au/ $\alpha$ -MoC Catalyst. *Nat. Catal.* **2023**, *6* (11), 1005–1015.
- (51) Qin, X.; Zhang, R.; Xu, M.; Xu, Y.; Zheng, L.; Li, C.; Yu, S.; Yan, J.; Xie, J.; Wu, G.; Rong, J.; Wang, M.; Ma, D. Selective Hydrogenation of Phenylacetylene by Carbon Monoxide and Water. *CCS Chem.* **2023**, *5* (10), 2358–2365.
- (52) Qin, X.; Xu, M.; Guan, J.; Feng, L.; Xu, Y.; Zheng, L.; Wang, M.; Zhao, J.-W.; Chen, J.-L.; Zhang, J.; Xie, J.; Yu, Z.; Zhang, R.; Li, X.; Liu, X.; Liu, J.-X.; Zheng, J.; Ma, D. Direct Conversion of CO and H<sub>2</sub>O to Hydrocarbons at Atmospheric Pressure Using a TiO<sub>2-x</sub>/Ni Photothermal Catalyst. *Nat. Energy* **2024**, *9* (2), 154–162.
- (53) Yang, M.; Li, S.; Wang, Y.; Herron, J. A.; Xu, Y.; Allard, L. F.; Lee, S.; Huang, J.; Mavrikakis, M.; Flytzani-Stephanopoulos, M. Catalytically Active Au-O(OH)<sub>x</sub>-Species Stabilized by Alkali Ions on Zeolites and Mesoporous Oxides. *Science* (1979) **2014**, *346* (6216), 1498–1501.
- (54) Yang, M.; Liu, J.; Lee, S.; Zugic, B.; Huang, J.; Allard, L. F.; Flytzani-Stephanopoulos, M. A Common Single-Site Pt(II)-O(OH)<sub>x</sub>-Species Stabilized by Sodium on “Active” and “Inert” Supports Catalyzes the Water-Gas Shift Reaction. *J. Am. Chem. Soc.* **2015**, *137* (10), 3470–3473.
- (55) Wang, L.; Wang, H.; Lu, J. Local Chemical Environment Effect in Single-Atom Catalysis. *Chem. Catal.* **2023**, *3* (4), No. 100492.
- (56) Babucci, M.; Guntida, A.; Gates, B. C. Atomically Dispersed Metals on Well-Defined Supports Including Zeolites and Metal–Organic Frameworks: Structure, Bonding, Reactivity, and Catalysis. *Chem. Rev.* **2020**, *120* (21), 11956–11985.
- (57) Jin, H.; Song, W.; Cao, C. An Overview of Metal Density Effects in Single-Atom Catalysts for Thermal Catalysis. *ACS Catal.* **2023**, *13* (22), 15126–15142.